

Exact Response Theory for Time-Dependent and Stochastic Perturbations

Original

Exact Response Theory for Time-Dependent and Stochastic Perturbations / Iannella, Leonardo; Rondoni, Lamberto. - In: ENTROPY. - ISSN 1099-4300. - ELETTRONICO. - 26:1(2024), pp. 1-23. [10.3390/e26010012]

Availability:

This version is available at: 11583/2987612 since: 2024-04-07T16:34:57Z

Publisher:

MDPI

Published

DOI:10.3390/e26010012

Terms of use:

This article is made available under terms and conditions as specified in the corresponding bibliographic description in the repository

Publisher copyright

(Article begins on next page)

A compression-shear fracture growing on an arch-gravity dam

Silvio Valente and Chiara Capriulo

Department of Structural, Geotechnical and Building Engineering, Politecnico di Torino, Italy

Qi He

College of Water Conservancy and Hydropower Engineering, Hohai University, China

Abstract

In the case of a narrow valley, characterized by a strong rock mass, the excavation can be designed according to the so called convergent way. In this case, the mean value of the compression stresses at the dam-foundation joint increases as the dam moves towards down-stream under the action of the water pressure applied to the up-stream side. During this slip settlement, the stress level in both materials, concrete and rock, remains allowable. It is true that the seismic load is able to increase such a slip displacement, nevertheless, since the structure is designed for horizontal hydrostatic loads, the stress level remains allowable even in such a seismic condition. The above mentioned issue was discussed during the 14th Benchmark Workshop on the Numerical Analysis of Dams organized by the International Commission on Large Dams (Stockholm, 6-9 September 2017). The theme B of the above mentioned Workshop was the static and seismic analysis of the Janneh dam. It is

¹Corresponding author: silvio.valente@polito.it

an arc-gravity dam, 157 meters high, now under construction in Lebanon, a high-seismicity region. The ten participants compared their results, obtained independently from each other and through different numerical models. In this paper the contribution of the authors is presented and the mechanical hypotheses at the base of the three-dimensional evolution of the crack path, at the dam-foundation joint, are discussed.

Keywords: Non-linear seismic analysis; Contact and friction; arch-gravity dam; interface crack; crack slipping displacement; crack opening displacement.

1. Highlights

- The simulation of the crack growth at the dam-foundation joint is necessary in order to predict the behaviour of a concrete dam realistically.
- Since the friction process is *dissipative*, the solution becomes *path-dependent* and a numerical *convergence* issue is faced.
- The convergent excavation is able to prevent the formation of tensile cracks in the lower part of the dam

2. Nomenclature

- a.s.l. : meters above sea level.
- b : length of a prismatic water element which is assumed as rigidly connected to the upstream face of the dam (Westergaard's model).
- formulators : the authors of reference [1], appointed by ICOLD to prepare the technical documents defining a theme of large interest.

- Creep: defined as the increase in deformation with time under constant load.
- H : free surface water level above the dam base
- ϵ_c : normal component of the concrete strain.
- ϕ_u : The ratio of the ultimate creep strain to the elastic strain , also called ultimate creep coefficient.
- \mathbf{n} : outgoing normal to the upstream surface of the dam.
- Pa : Pascal [*Newton/m²*]
- σ_c : normal component of the concrete stress (pressure).
- σ_n : pressure normal to the dam/foundation interface.
- τ : tangential stress at the dam/foundation interface.
- γ : tangential component of the displacement discontinuity at the dam/foundation interface.
- \ddot{u}_g : dam base acceleration.
- Z : Westergaard's element level above the dam base.

3. Introduction

Dam-foundation interaction is a highly non-linear contact problem. In order to solve this problem many methods were proposed in the mathematical literature (see [2]). The state of the art on the engineering treatment

of such methods is reported in the book of Wriggers [3]. In order to compare the results that can be obtained by applying this large base of knowledge in a specific case, the Technical Committee A of the International Commission On Large Dam (shortened ICOLD) accepted the case study proposed by Artelia Eau & Environnement as the subject of the theme B of the 14th International Benchmark Workshop on Numerical Analysis of Dams [1]. This case study was the Janneh dam (157 m high, see Figures 1 and 2), now under construction in Lebanon, a high-seismicity region.

Each participant worked independently, on the same geometrical and mechanical data given by the formulators.

Since the valley is narrow and the strength of the bedrock is high (ultimate compression strength 50 MPa), the designer (A.Yziquel [4]) decided to use a curve layout in order to trigger the arch effect, even under normal operating conditions. The arch effect transfers a part of the water pressure to the abutments of the dam laterally. Under seismic load this choice prevents from an unacceptable sliding of the dam on its foundation. In order to prevent the tensile cracking of the dam, a convergent excavation was used (see Figure 3). Furthermore, the downstream slope of an arch-gravity dam may be steeper than that of a straight gravity dam. As a consequence, less concrete is necessary.

4. Geometry of the dam

For the purpose of saving concrete and excavation volume, the downstream toe of the dam has been vertically-truncated. Due to this feature, the 2D section of the central block does not satisfy the generally adopted

Parameters	Value
Maximum height above excavation	157 m
Width at the crest	10 m
Maximum width at the base	66 m approx
Crest length	300 m approx
Radius of curvature of the upstream face	240 m
Elevation of the crest	847 m
Elevation of the spillway	839 m
Ratio Horizontal/Vertical projection of the downstream slope in the upper part of the dam	0.8

Table 1: Main features of the Janneh dam (from [1])

stability criteria for straight gravity dam. The stability of the dam relies consequently on its 3D behaviour. The definition of the upstream and downstream faces of the dam is cylindrical (simple curvature). The main features of the Janneh dam are provided in Table 1.

5. Types of analysis

The calculation required to the participants follows a progressive approach: the subsequent stages are of increasing complexity. The concrete and the bedrock always follow a linear elastic constitutive law. The analyses based on a non-linear behaviour of the dam/foundation interface are discussed in this paper. The material properties assumed are shown in Table

Material	Density	Static deform. modulus	Dynamic deform. modulus	Poisson ratio	Cohesion	Coulomb friction angle	Tensile strength
	[kg/m^3]	[GPa]	[GPa]	-	[Pa]	-	[Pa]
Concrete	2400	20	30	0.2			
Bedrock	2800	25	30	0.25			
Dam/ foundation interface					0	$\pi/4$	0

Table 2: Material properties.

Since the friction process is *dissipative*, the solution becomes *path-dependent* and a numerical *convergence* issue is faced.

The stresses induced by each construction stage have to be added to the stress level achieved at the end of the previous stage.

6. The friction model at the interface

Both materials, concrete and rock, behave in a linear elastic way. The dam-foundation interface follows the Coulomb friction law:

When the interface is closed:

$$\text{if } |\tau|/\sigma_n < 1 \text{ then it is } \dot{\gamma} = 0 \quad (\textit{sticking condition})$$

$$\text{else } |\tau| = \sigma_n, \dot{\gamma} \neq 0 \text{ and } \dot{\gamma}\tau > 0 \quad (\textit{slipping condition})$$

When the interface is open:

$$\tau = \sigma_n = 0$$

where γ is the sliding discontinuity, and σ_n is the effective normal stress.

Therefore the non-linear behaviour only occurs at the interface and its analysis is formulated as an *incremental problem* (overdot means time derivative). In this work a *node-to-surface* contact method is used (see [3]). Since the expected maximum value of the sliding displacement is 5 mm and, in the model analysed, the minimum side of the surface triangular elements is 1227 mm, a small sliding formulation is used. In order to enforce the contact constraint, a penalty method is used. According to this method, in the optimization problem, a penalty function is added to the objective function. This term consists of a penalty parameter multiplied by a measure of violation of the constraints (see [2]).

When the Newton-Raphson method is applied to a contact with friction problem, a loss of convergence sometimes occurs [5]. To prevent a large number of sticking-to-slipping transitions, when the slipping displacement increment is less than 0.2 mm, the interface behaviour is assumed as adhesion.

Some other participants to the benchmark used the so called '*mortar method*' or the '*cohesive crack model*'. This is the main origin of scattering in the results shown in Figures 4 and 5, due to bifurcations phenomena occurring in the equilibrium path (see reference [6] and [7])

The results presented in this paper are obtained through the ABAQUS code [8]. The friction condition is applied starting from the batch of the first layer.

7. Self-weight calculation

The dam is made of Roller Compacted Concrete (RCC). Moreover, the downstream slope of Janneh dam is steeper than that one of a straight gravity dam, which makes it more sensitive to sequential changes of structural

system during construction. In this study, a time step of 56 days is used to simulate each of the 10 approximated layers of construction (see Figure 6). The relationship of time dependent strain model $\epsilon(t)$ due to the varying load scheme is given by :

$$\epsilon(t) = \epsilon_{el}(t) + \epsilon_c(t) \quad (1)$$

Where:

$$\epsilon_{el}(t) = \frac{\sigma(t)}{E_{cm}} \quad (2)$$

Where $E_{cm} = 30GPa$ is the instantaneous elastic modulus given by Table 2 and $\sigma(t)$ is the stress history given by the load due to the layer construction stages. In order to simplify the benchmark, the formulators assumed the following unchallengeable hypotheses:

- the thermal effects and shrinkage are neglected.
- the construction time is not specified and the creep model to use is up to each participant.

Following the Model Code 2010 [9], assuming $t_0 = 28$ days, under a constant σ_c , the creep strain ϵ_c in this work evolves as follows:

$$\epsilon(t - t_0) = \frac{\sigma_c}{E_{cm}} \phi(t - t_0) \quad (3)$$

Where $\phi(t - t_0)$ is given according to eq. 5.1-71a in reference [9]:

$$\phi(t - t_0) = \phi_u \left(\frac{t - t_0}{350 + (t - t_0)} \right)^{0.3} \quad (4)$$

In the absence of specific creep data for local aggregates and conditions, the ultimate creep coefficient was assumed according to equation A-19 in reference [10] ($\phi_u = 2.35$). The principle of superposition is assumed to be valid ([11] and [12]), and the viscoelastic model is based on a Prony series representation [8] of creep data based on reference [9]. Further details on the time dependent model for concrete are presented on [9].

The self-weight of each of the ten above mentioned layers is applied linearly over the related 56 days of time. The evolution of the pressure in a central point of the dam/foundation interface is shown in Figure 7

At the end of the self-weight calculation, all the displacements of the model are reset to zero.

8. Static analysis

The static analysis is carried out for Normal Water Level (shortened NWL) at 839 m a.s.l. The downstream water level is considered at the bedrock level: 685 m.a.s.l.. Due to its thickness, the effect of uplift is significant on the dam stability. If a well penetrates the dam, water will rise to the level of the so called 'piezometric line' or 'water table'. A drainage efficiency equal to 1/3 is considered 10 m behind the upstream face of the dam. It means that the drainage is able to reduce the total water pressure, which is due to a water column of $839 - 685 = 154$ m., to 1/3 of its value. Therefore the piezometric line intersects with the drainage at level $685 + 154/3 = 736.33$ m.a.s.l. The uplift distribution is shown in Figure 8 and it is assumed as independent on the open region of the dam/foundation interface. The uplift is applied to the dam as external forces.

Figures 4 and 5 show the results obtained by the ten participants to the benchmark, independently (see [1]). The contribution described in this paper is labeled P9. The curve called 'Reference' is obtained by the formulators and it is not known to the participants during the preparation of their own contribution. The main reason of variability in the results are:

- The choice of the creep and crack model is up to each participant.
- Only the solid model is unique between the participants. The choice of the finite element used is up to each participant.
- The Reference solution is obtained through the Finite Difference Method, all the other solutions are obtained through the Finite Element Method.

More details on the hypotheses assumed by the other participants are described in their own contribution, published in the conference proceedings. The corresponding author of each contribution is listed as author of reference [13].

9. Seismic analysis

The earthquake response of an arch dam is influenced by its dynamic interaction with foundation rock and the impounded water [14]. The calculations are based on the above mentioned non-linear model, whose results are considered as the initial state. The pseudo-static analysis is carried out considering the following:

- The seismic inertia load is applied statically toward downstream. A second case, based on inertia load applied toward upstream, is discussed in [15] and not repeated here;

- The response spectrum is a plot of the peak response (pseudo-displacement, pseudo-velocity or pseudo-acceleration) of a series of oscillators of varying natural period, as a function of their natural period.
- In this specific case the oscillator damping was assumed as 5% of the critical value
- Only the horizontal component of the inertia forces are considered.
- The hydrodynamic pressure is calculated according to Westergaard's approach [16, 17] ; The shaded area in Figure 9 is a water prismatic element which is assumed to be rigidly connected to the upstream surface of the dam. Therefore the water/dam interaction is formulated in a local reference system which is variable from point to point on the upstream surface of the dam. Each prismatic element is assumed to be independent from the others. According to the above mentioned hypotheses, a lumped mass is added to the mass matrix of the dam.
- The foundation is considered massless;
- The normal water level at 839 m a.s.l. is assumed;
- The 3D mesh is based on continuum elements with four nodes for both materials: concrete and rock. The choice of tetrahedral elements is due to its higher capacity to mesh such a complex geometry.
- The interface condition is contact with friction. It is true that the incremental process up to this construction stage and load level is non-linear, but, before extracting the eigenvalues, the system behaviour is linearized in the vicinity of the reached configuration.

With the above mentioned hypotheses, the fundamental period of the dam/foundation/ reservoir system is 0.39 s (see Figure 10) and its modal mass is equal to 57.8% of the total mass. The related pseudo-acceleration is $6.65m/s^2$. The acceleration site response spectrum is given by the formulators (see Figure 11). Lower and higher bounds are respectively the minimum and the maximum value of the fundamental period obtained by the participants to the benchmark.

Figure 12 shows the real crack tip front line induced by the above mentioned pseudo-static horizontal forces. The interface points placed upstream of this line are open, the others are closed. With reference to the closed part of the interface, the square size in Figure 13 is proportional to the ratio τ/σ_n . According to the friction angle shown in Table 2, when this ratio achieves the value 1, a slipping displacement can occur.

Figure 14 shows the tensile stresses induced on the rock mass by the seismic load. The maximum local value is 1.812 MPa, allowable for a material characterized by an ultimate compression strength of 50 MPa.

10. Conclusions

- The simulation of the crack growth at the dam-foundation joint is necessary in order to predict the behaviour of a concrete dam realistically.
- Since the friction process is *dissipative*, the solution becomes *path-dependent* and a numerical *convergence* issue is faced.
- The convergent excavation is able to prevent the formation of tensile cracks in the lower part of the dam

- The tensile stresses induced in the rock mass are allowable.

11. Funding

This work was supported by the Politecnico di Torino [grant number 57_RBA17VALSIL]; Italian Super Computing Resource Allocation of CINECA [grant number IsC49_icold_bw].

12. References

- [1] F. Andrian, P. Agresti, G. Mathieu, Theme b synthesis report: Static and seismic analysis of an arch-gravity dam, in: R. Malm, M. Hassanzadeh, R.Hellgren (Eds.), Proceedings of 14th ICOLD International Benchmark Workshop on Numerical Analysis of Dams, KTH, 2018, pp. 240–393, <http://kth.diva-portal.org/smash/get/diva2:1186453/FULLTEXT01.pdf>.
- [2] N.Kikuchi, J.T.Oden, Contact problems in elasticity: a study of variational inequalities and finite element methods, SIAM, Society for Industrial and Applied Mathematics, Philadelphia, USA, 1988, ISBN 0-89871-468-0.
- [3] P. Wriggers, Computational Contact Mechanics, Springer, Berlin, Heidelberg, New York, 2006, ISBN 978-3-540-32609-0, Second edition.
- [4] A. Yziquel, F. Andrian, P. Agresti, Janneh dam project non-linear simulation of an arch gravity dam, in: Proceedings of 13th ICOLD International Benchmark Workshop on Numerical Analysis of Dams, Lausanne, Switzerland, 2015, pp. 371–380.

- [5] S. Valente, A. Alberto, F. Barpi, A large time increment method applied to an interface cohesive crack growing in compression-shear conditions, *Engineering Fracture Mechanics*, ISSN: 0013-7944, doi: 10.1016/j.engfracmech.2016.04.019.
- [6] S. Valente, Bifurcation phenomena in cohesive crack propagation, *Computers and Structures* 44 (1/2) (1992) 55–62.
- [7] F. Barpi, S. Valente, M. Cravero, G. Iabichino, C. Fidelibus, Fracture mechanics characterization of an anisotropic geomaterial, *Engineering Fracture Mechanics* 84 (2012) 111–122, ISSN: 0013-7944, doi:10.1016/j.engfracmech.2012.01.010.
- [8] Dassault, Systemes, SIMULIA, Corp. (Eds.), Abaqus 6.14 documentation, Johnston, RI 02919, USA, 2017, <http://130.149.89.49:2080/v6.14/index.html>.
- [9] International, Federation, Structural, Concrete (Eds.), Model Code for Concrete Structures, Ernst & Sohn, a Wiley Brand, Berlin, Germany, 2010, ISBN: 978-3-433-03061-5, www.fib-international.org/fib-model-code-2010.
- [10] Committee, 209 (Eds.), Guide for Modelling and Calculating Shrinkage and Creep in Hardened Concrete, American Concrete Institute, Farmington Hills MI, USA, 2008.
- [11] F. Barpi, G. Ferrara, L. Imperato, S. Valente, Lifetime of concrete dam models under constant loads, *Materials and Structures* 32 (1999) 103–111, ISSN: 13595997.

- [12] F. Barpi, S. Valente, Fuzzy parameters analysis of time-dependent fracture of concrete dam models, *International Journal for Numerical and Analytical Methods in Geomechanics* 26 (2002) 1005–1027, doi: 10.1002/nag.235.
- [13] G. Faggiani, S. Fray, L. Gracia, A. Kollatou, S. Mitovski, E. Robbe, J. Salamon, E. Staudacher, S. Teodori, S. Valente, Theme 'b': Static and seismic analysis of an arch-gravity dam, in: R. Malm, M. Hassanzadeh, R.Hellgren (Eds.), *Proceedings of 14th ICOLD International Benchmark Workshop on Numerical Analysis of Dams*, KTH, 2018, pp. 287–393, <http://kth.diva-portal.org/smash/get/diva2:1186453/FULLTEXT01.pdf>.
- [14] A. Chopra, *Dynamic of structures*, Prentice Hall, Upper Saddle River, New Jersey, USA, 2012, iSBN 13: 978-0-13-285803-8, Fourth edition.
- [15] S. Valente, C. Capriulo, Theme b: Static and seismic analysis of an arch-gravity dam, in: R. Malm, M. Hassanzadeh, R.Hellgren (Eds.), *Proceedings of 14th ICOLD International Benchmark Workshop on Numerical Analysis of Dams*, KTH, 2018, pp. 287–296, <http://kth.diva-portal.org/smash/get/diva2:1186453/FULLTEXT01.pdf>.
- [16] USA, Army, Corps, Engineers (Eds.), *Theoretical Manual for Analysis of Arch Dams*, Technical Report ITL-93-1, Emeryville, CA., USA, 1993, <http://www.dtic.mil/dtic/tr/fulltext/u2/a269524.pdf>.
- [17] USA, Army, Corps, Engineers (Eds.), *Time History Dynamic Analysis of Concrete Hydraulic Structures*, EM No. 1110-2- 6051, Washington,

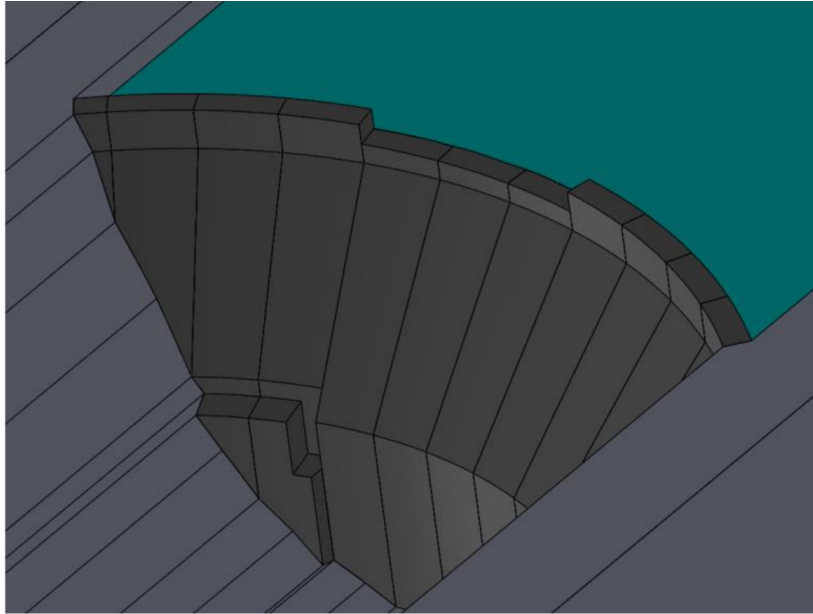


Figure 1: Janneh dam: dam-foundation solid model (from [1])

DC, USA, 2003, <http://www.publications.usace.army.mil/Portals/76/Publications/EngineerManuals/EM-1110-2-6051.pdf?ver=2013-09-04-102314-930>.

- [18] E. Staudacher, G. Zenz, Theme b: Static and seismic analysis of an arch-gravity dam, in: R. Malm, M. Hassanzadeh, R. Hellgren (Eds.), Proceedings of 14th ICOLD International Benchmark Workshop on Numerical Analysis of Dams, KTH, 2018, <http://kth.diva-portal.org/smash/get/diva2:1186453/FULLTEXT01.pdf>.

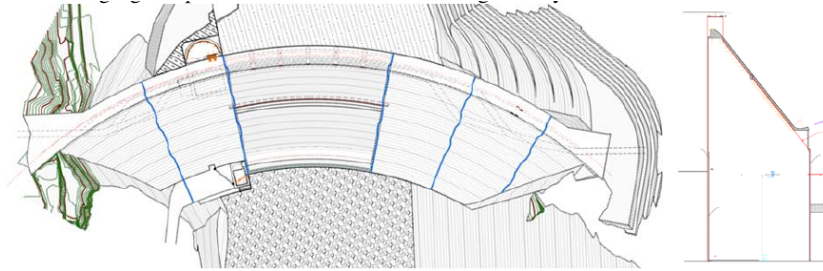


Figure 2: Janneh dam: plane view and cross section of the central block (from [1])

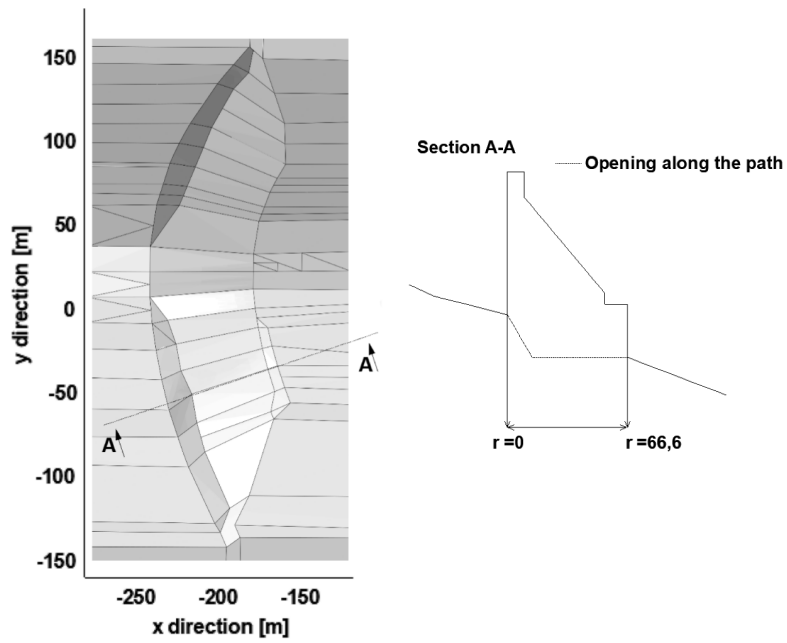


Figure 3: Janneh dam: convergent excavation (from [1])

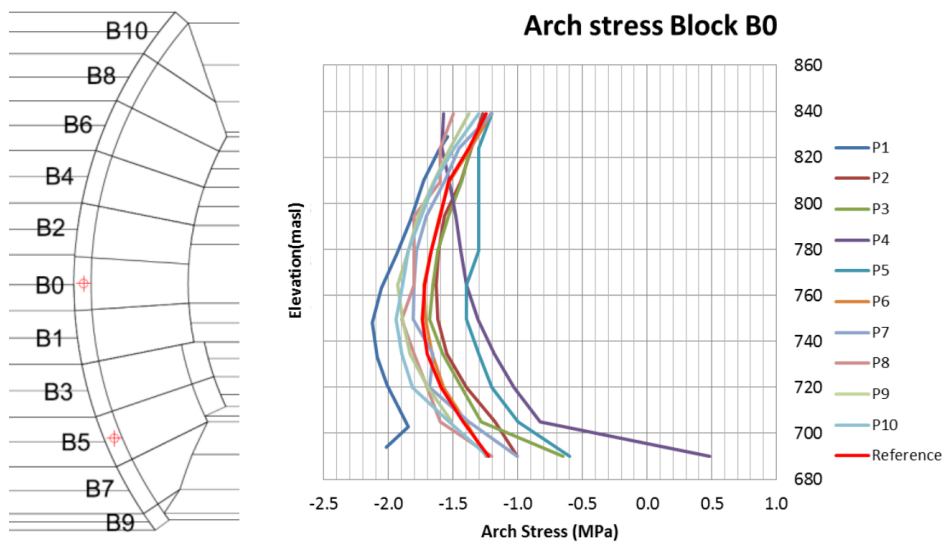


Figure 4: Arch stress due to Normal Water Level 839 m a.s.l (from [1])

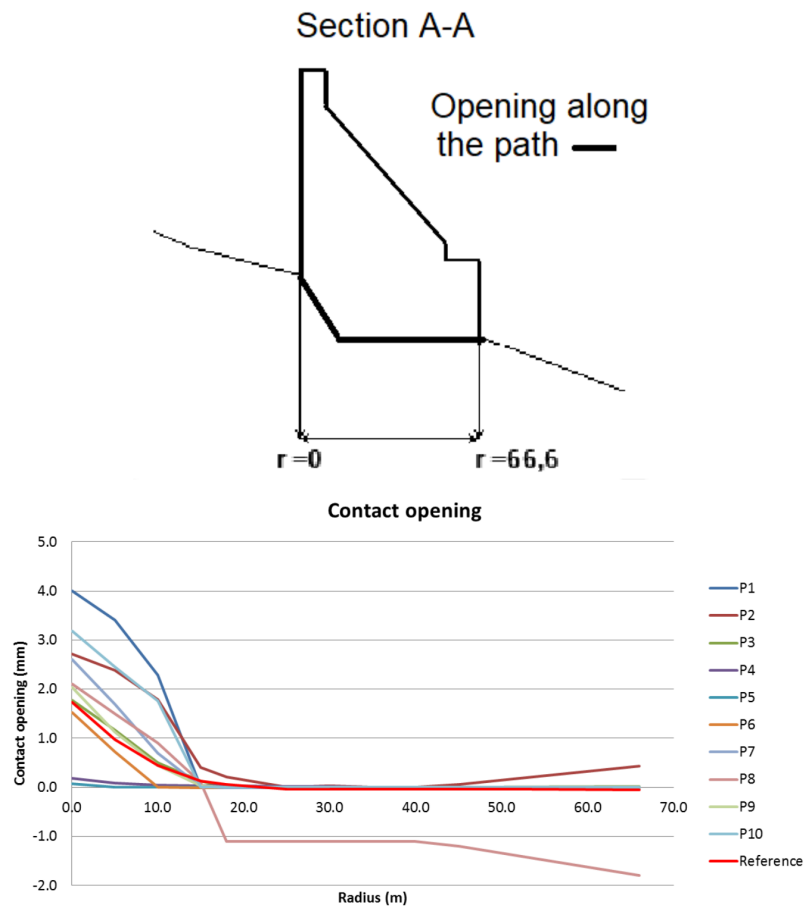


Figure 5: Static non-linear analysis for the Normal Water Level: crack opening displacements (from [1])

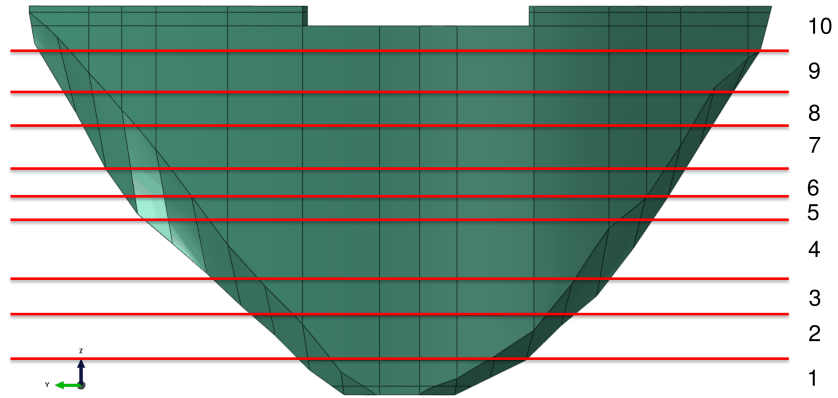


Figure 6: Ten construction stages (from [18])

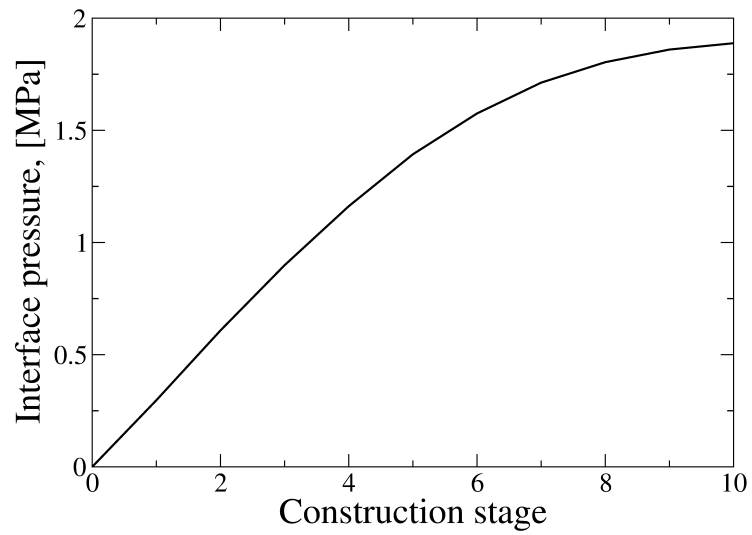


Figure 7: Pressure in a central point of the dam/foundation interface

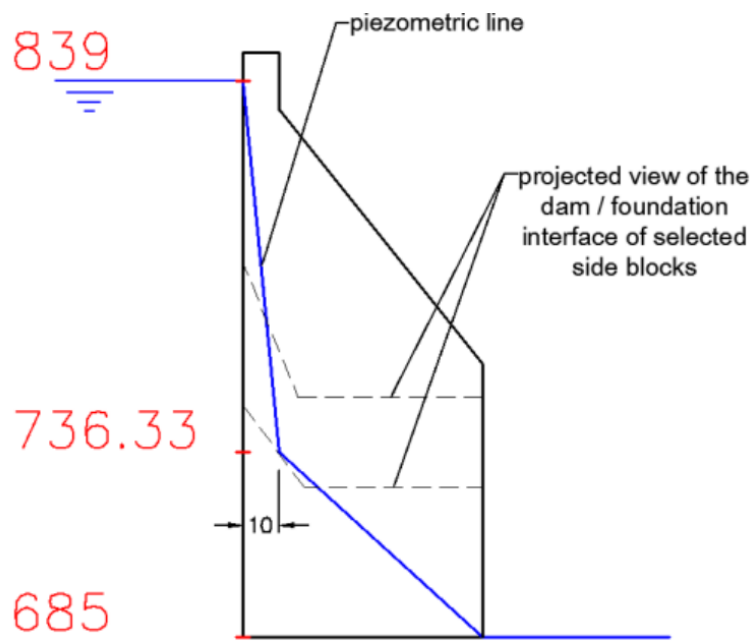


Figure 8: Uplift pressure across the dam (from [1]); the length unit is meter; the numbers on the left side are quoted a.s.l.

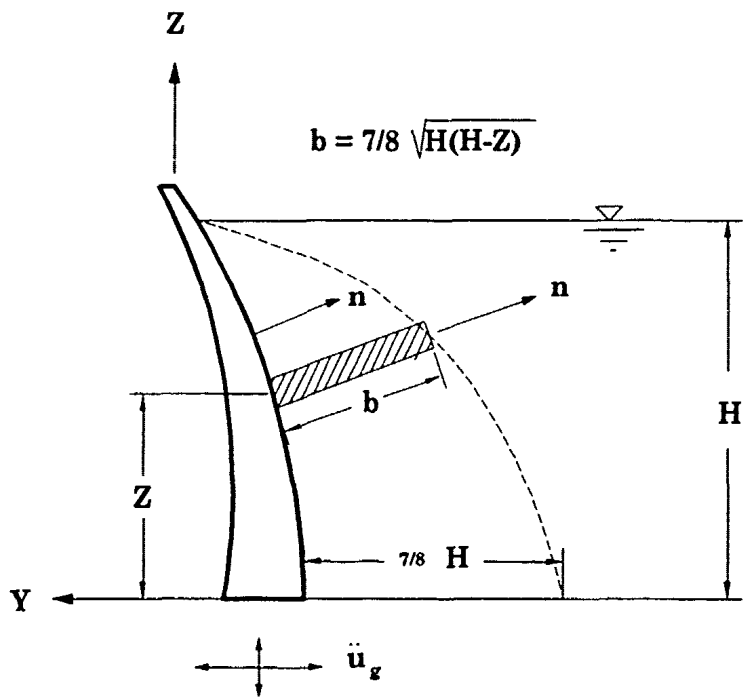


Figure 9: Westergaard's added-mass representation for arch dams (from [16])

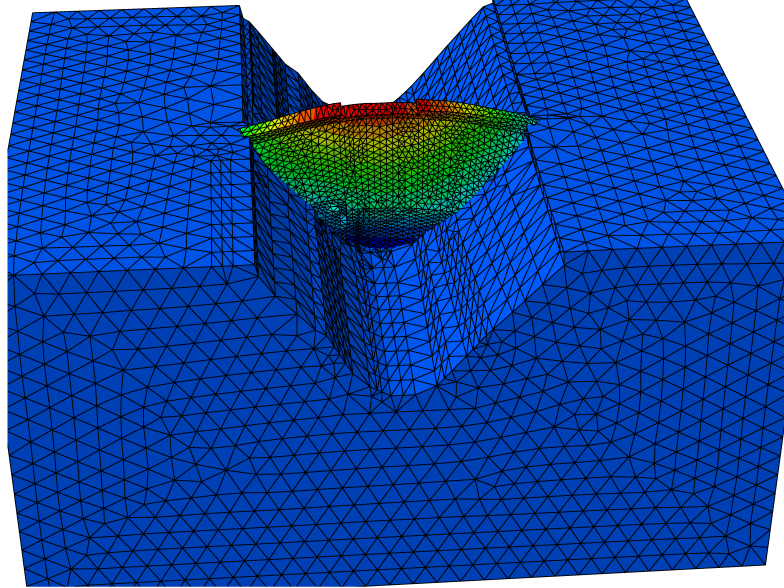


Figure 10: First eigenvalue for the system linearized at the Normal Water Level

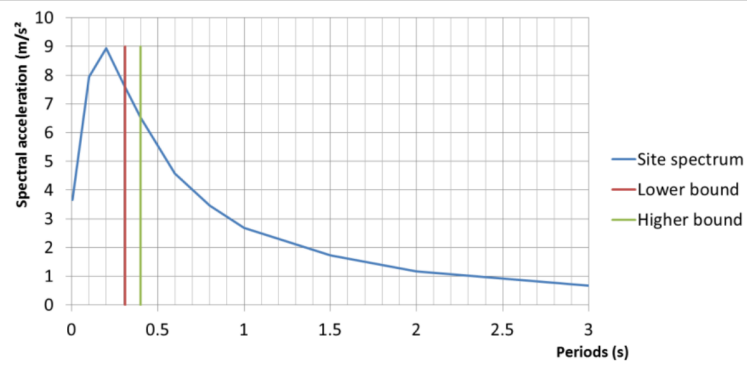


Figure 11: Pseudo-acceleration site response spectrum (from [1])

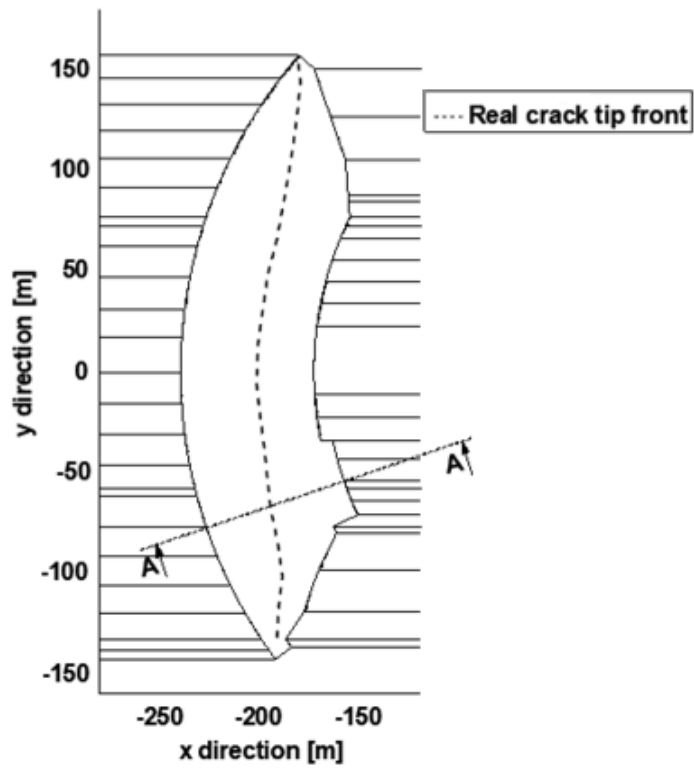


Figure 12: Real crack tip front

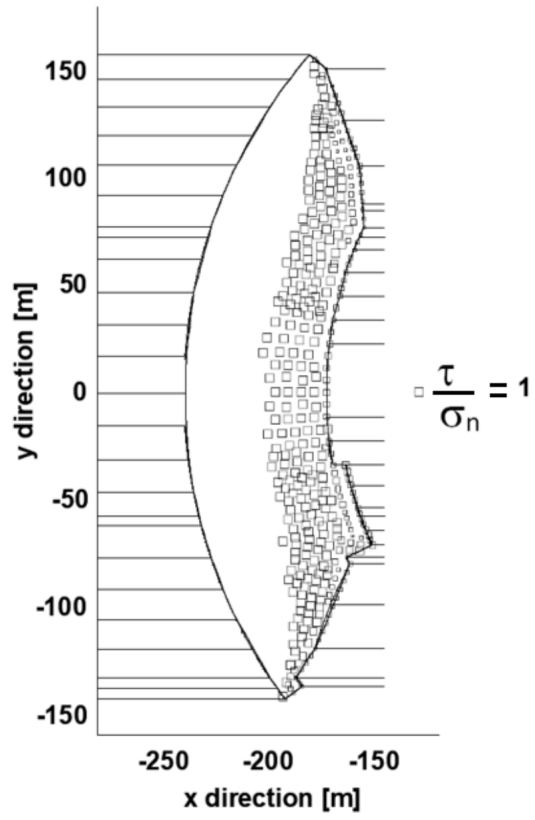


Figure 13: Crack path at the interface induced by inertia forces toward downstream

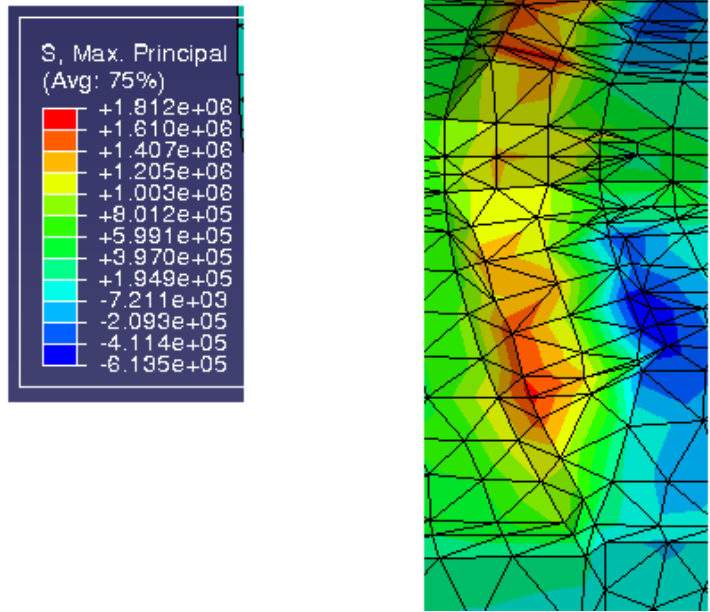


Figure 14: Tensile principal stress induced in the bedrock [Pa]